

Kinetics, Equilibrium and Thermodynamic Studies of Mn (II) Biosorption from Aqueous Solution onto *Pleurotus Ostreatus*

Abdul Naeem* Afsar Khan, Tahira Mahmood, Mairman Muska, Salah Ud Din,
Muhammad Saleem Khan¹, Muhammad Hamayun and Muhammad Waseem

National Centre of Excellence in Physical Chemistry, University of Peshawar, Peshawar. 25120, Pakistan.

¹Department of Botany, Islamia College University, Peshawar.

naeem64@yahoo.com*

(Received on 7th May 2013, accepted in revised form 7th January 2014)

Summary: Biosorption of Mn (II) from aqueous solution by *P. Ostreatus* was investigated at different concentrations, pH and temperature. The close agreement between the experimental and theoretical biosorption capacity confirmed that Pseudo 2nd order equation is best fitted to the present experimental data. The biosorption capacity of *P. Ostreatus* was observed to be dependent upon the pH and temperature of adsorption system. The values of biosorption maxima (X_m) and binding energy constant (K_b) were observed to decrease with rise in temperature in the range of 298 – 323K. The negative values of ΔG and ΔH showed the process of Mn (II) biosorption onto *P. Ostreatus* is spontaneous and exothermic respectively. Similarly, the values of isosteric heat of biosorption ($\overline{\Delta H}$) were decreased with increase in surface coverage (θ) which indicated that the surface of the *P. Ostreatus* is energetically heterogeneous in nature.

Keywords: *P. Ostreatus*, Mn (II), Langmuir isotherm, Thermodynamic parameters, Isosteric heat of adsorption.

Introduction

Several environmental issues have been raised with the industrial revolution in the last two decades. Contamination of drinking water by toxic metals is one of the emerging problems all over the world [1- 2]. The excess of these heavy metals concentration in the water body causes serious threats to human body as well as to micro-organisms in the water [3]. Various industries including plastic, electroplating, storage batteries, mining and metallurgical industries are mainly responsible for the contamination of water [4 - 6]. Manganese may be found in one of the oxidation states of +2, +3, +4, +6, or +7 but it is abundantly available in water samples in +2 oxidation state being the most stable state [7]. It is basically found in both organic and inorganic forms. Inorganic manganese is used in steel, battery, ceramics and dietary products while organic manganese is used in pesticides, fertilizers and as anti knocking agent in gasoline. According to water quality standard, the permissible limit for manganese is 0.5 mg L⁻¹ [8]. Occupational and environmental exposure to Mn (II) disturbs the central nervous system. Manganese causes different diseases such as Manganism [muscle stiffness, lack of coordination, tremors, difficulties with swelling and breathing], learning disabilities and liver problems in children, male fertility and birth defects *i.e.* short tails, low external ears [9].

As a reducing agent Mn (II) raises the Chemical Oxygen Demand (COD), which in turn

affects the water quality for aquatic life. The large number of electrons in acidic soil facilitates the Mn (II) solubility in water which becomes toxic to the soil crops [10].

The highest level [2.56 mg L⁻¹] of Mn (II) in Charsada and Risalpur of Khyber Pakhtunkhwa was reported by [11, 12]. Mn (II) in ground water of Faisalabad was reported to be 1.06 mg L⁻¹. In many other parts of Pakistan Mn (II) is found to exceed its permissible limit which include Hayat Abad, Akbar Pura, Hasan Abdal, Gadoon, Palosi drain of Peshawar, Kalanwala, Kalar Kahar, Kasur and Sialkot City of Punjab, Korangi, Sehwan, Machar Lake Jamshoro of Sindh in Pakistan [13].

Resources of manganese in Pakistan are mostly found in Hazara, Kuram Agency, Bajawaur and North Waziristan of Khyber Pakhtunkhwa. It is also found in Lasbela and Khusdar districts of Baluchistan. Sources of manganese are available in Sanjro, Dhora, Kalat, Khabri and Dadi Dhora of Sindh province. Total resources of manganese are 11 million tons with average of 45 % MnO found in Hazara.

Metal ions are generally removed from the water by several methods such as reverse osmosis, ultra filtration, electro dialysis, ion-exchange, chemical precipitation, phytoremediation and solvent extraction. Some of the disadvantages of these traditional methods are sludge formation, use of large

*To whom all correspondence should be addressed.

amounts of chemicals, addition of anti precipitants, need of replacement of membranes and more electricity, and only physical kind of separation [14-16]. Biosorption is a new technology which is preferably tested for the uptake of many toxic pollutants from drinking water because of its its high efficiency, low cost, no requirements of additional chemicals, minimization of chemical and biological slugs, regeneration of biosorbents and possibility of metals recovery [17]. Various biosorbents such as aliginat gel bead, kaolinite, agaricus bisporous, boliyus edulis and russula delica have been tested for the recovery of heavy metals from water. Some of these adsorbents have low adsorption capacity and low stability in a natural environment [18].

Macro fungus may be found easily in many places of the world and have a good stability in both the acidic and basic medium [19]. Mushroom family was found to be best biosorbents for removal of heavy metals and can be grown in natural habitat [20]. *P. Ostreatus* is an edible mushroom and has been chosen for Mn (II) adsorption from aqueous solution because of its easy availability, fast kinetics and high adsorption capacity.

Results and Discussion

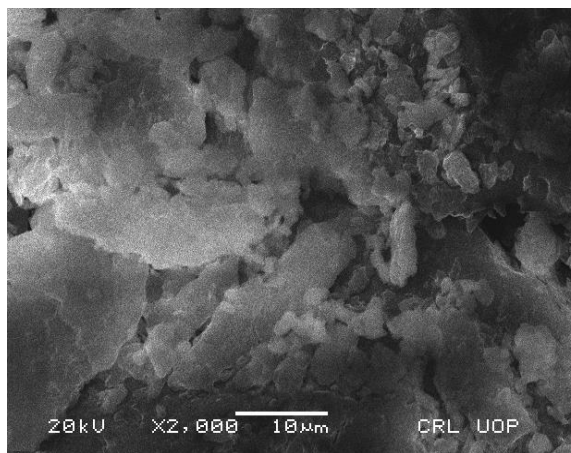
Characterization of *P. Ostreatus*

Scanning Electron Microscopy / Energy Dispersive X-ray (SEM/EDX)

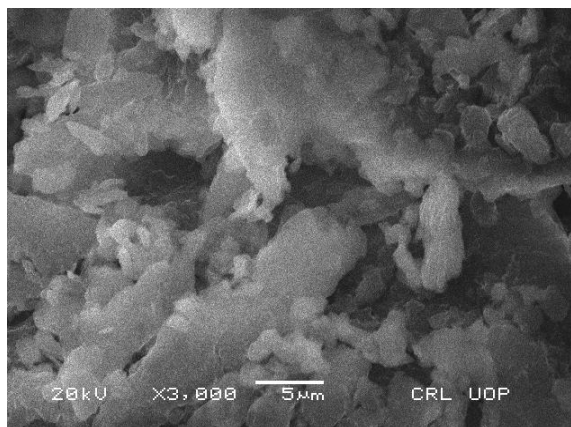
The scanning electron microscopy (SEM) micrograph recorded for *P. Ostreatus* surface are given in Fig. 1 The images show that the surface of *P. Ostreatus* is irregular in shape and porous in nature. The porous nature of the surface indicates the mushroom to be a suitable biosorbent for the decontamination of water. The EDX spectra (Fig. 2) of *P. Ostreatus* show that carbon and oxygen are the major elements in addition to K. The weight percent of C, O and K are recorded to be 51.7, 46.3, and 2.26 % respectively. These results are comparable with findings reported by [21].

Surface Area

The surface area of *P. Ostreatus* is observed to be $81 \text{ m}^2 \text{ g}^{-1}$ which is sufficiently greater than the surface area ($3.7 \text{ m}^2 \text{ g}^{-1}$) reported by [22], for the same species. The current value of surface area is comparable with that reported by [23] for some other biosorbent.



A



B

Fig.1: SEM images of *P. Ostreatus* at (A) 2000 Xs (B) at 3000 Xs.

Thermogravimetric / Differential thermal analysis (TG/DTA)

TG/DTA analysis of *P. Ostreatus* reveals the total weight loss to be 93 % which was observed to occur in three stages (Fig. 3). The first weight loss of 18% occurred in the temperature range of 50 to 250 °C which is assigned to the dehydration of the biomass. The second weight loss of 43 % upto 390 °C is due to the conversion of organic matter to atmospheric gases *i.e.* CO₂ and CO etc [24]. The third weight loss of 31 % may be due to the passive pyrolysis till 900 °C. Similar TG results were reported by [25], while studying the thermal behavior of different fungi.

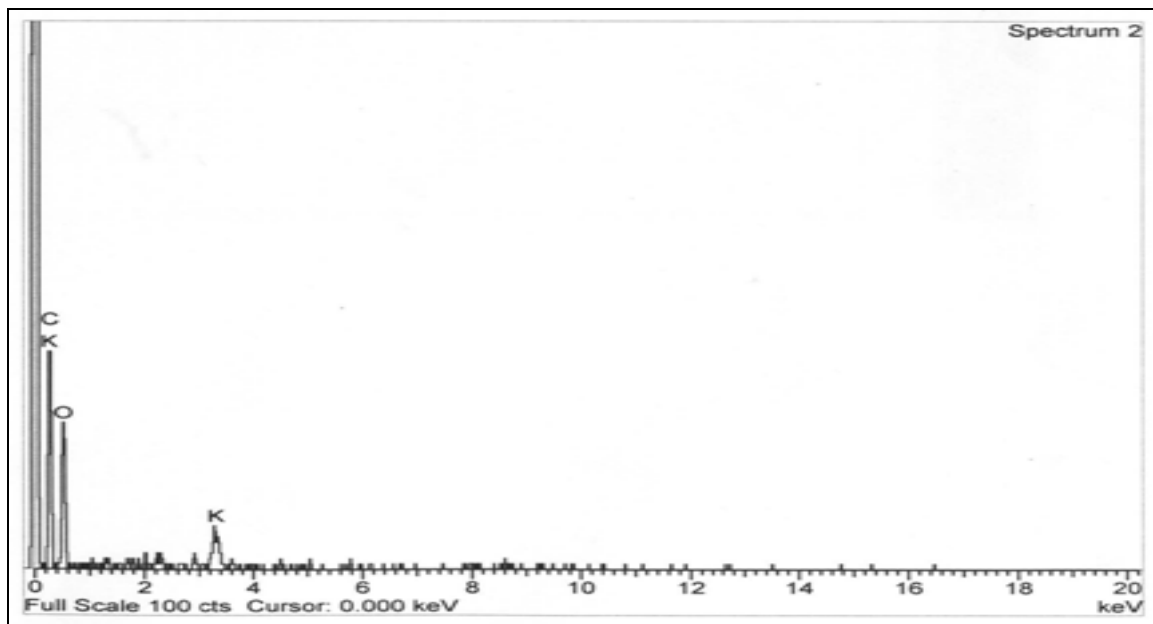


Fig. 2: Energy dispersive X-ray of P. Ostreatus.

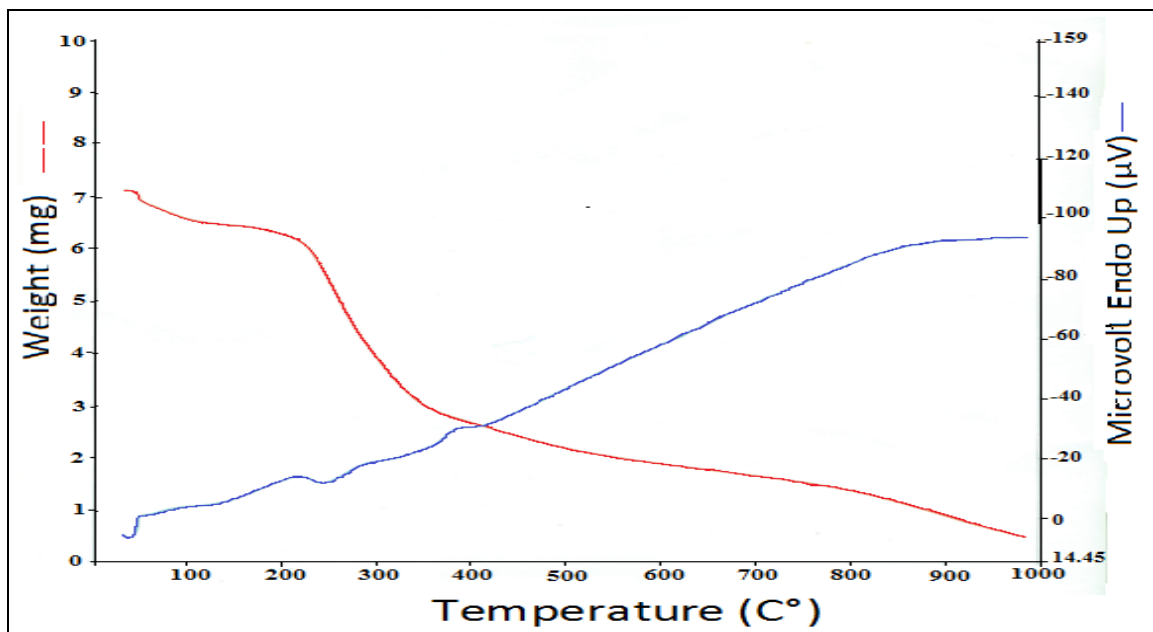


Fig. 3: Thermogravimetric / Differential thermal analysis of P. Ostreatus.

Fourier Transforms Infrared Spectroscopy (FTIR)

FTIR spectrum of P. Ostreatus has been shown in the Fig. 4 (A). The sorption band in the range of $3500 - 3000 \text{ cm}^{-1}$ generally indicates the OH group of carbohydrate (glucose) and NH_2 group of proteins [26]. The absorption band at 2900 cm^{-1} shows the -CH stretching vibration. The weak absorption band at 1600 cm^{-1} is attributed to C = O

group of proteins. Similarly the band at 1050 cm^{-1} is assignable to C - O - C stretching vibration.

Point of Zero Charge (PZC)

The PZC of P. Ostreatus determined by salt addition method [27] was found to be at pH 6.5 (Fig. 5) which is close to the value (6.1) reported for cupressus cones [28].

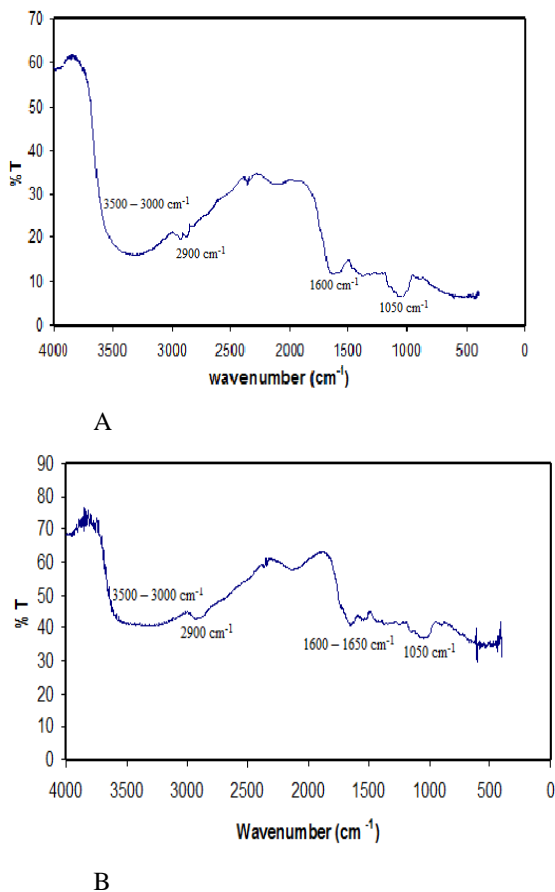


Fig. 4: FTIR spectra of P. Ostreatus (A) before (B) after sorption of Mn (II).

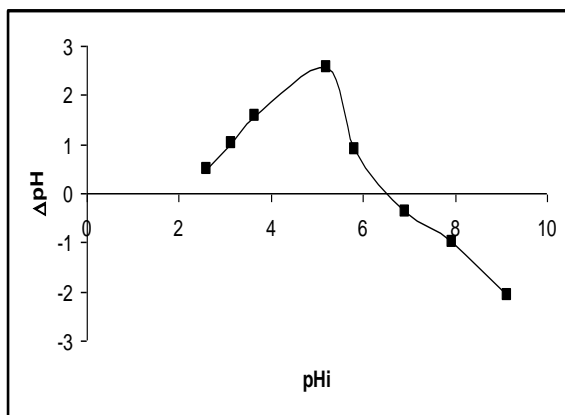


Fig. 5: Point of zero charge (PZC) of P. Ostreatus at 298 K.

Effect of Contact Time on Mn (II) Adsorption

Adsorption of Mn (II) from aqueous solution onto P. Ostreatus was studied at different intervals of time at 298 K in this study. The amount of Mn (II)

sorbed in (mol g^{-1}) is plotted vs. time (Fig. 6). The uptake of Mn (II) onto P. Ostreatus increases with time and reaches to maximum adsorption in 120 min and no further uptake of Mn (II) observed after equilibrium. The graphical data also reveals that more than 90% adsorption of Mn (II) onto P. Ostreatus takes place in the first 5 min. The rapid adsorption of Mn (II) points towards the favorability of the P. Ostreatus for the decontamination of water. Almost similar results were reported by [8] while studying sorption of Mn (II) onto activated carbon at pH 4.

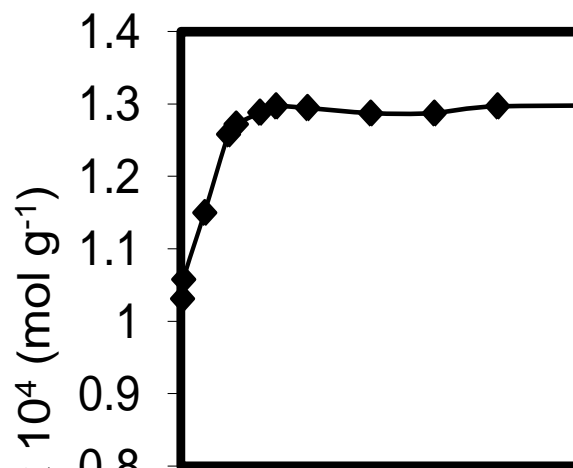


Fig. 6: Kinetic study of Mn (II) sorption onto P. Ostreatus at 298K and pH 7.

Kinetic Modeling

Kinetic model is generally used to elucidate the mechanism of adsorption. The linear form of pseudo 1st and pseudo 2nd order models were applied to interpret the current kinetic data. The pseudo first order model [18] was found to be inapplicable to the current experimental data. Thus the pseudo second order kinetic model in the following form was preferably used

$$\frac{t}{q_t} = \frac{1}{k_2 q_e^2} + \frac{t}{q_e} \quad (1)$$

where q_t (mol g^{-1}) is the sorbed metal ions at time (t), q_e (mol g^{-1}) is sorbed metal ions at equilibrium, k_2 ($\text{g min}^{-1} \text{mol}^{-1}$) is 2nd order rate constant. Plot of t/q_t vs. t (Fig. 7) gives straight line with $R^2 = 1$ indicating that the Pseudo second order model is well

fitted to the kinetic data. Moreover, a close agreement between experimental and theoretical sorption capacity (q_e) also validates that this model is the best choice (Table-1). The applicability of pseudo second order model shows the sorption of Mn (II) is chemical in nature [29].

Table-1: Kinetic parameters for Mn (II) biosorption onto P. Ostreatus at 298 K and at pH 6.

Temp (K)	$q_e \times 10^3$ (mol g ⁻¹) (experimental)	$q_e \times 10^4$ (mol g ⁻¹) (theoretical)	K_2 (g min ⁻¹ mol ⁻¹)	R ²
298	1.29	1.29	3677	1

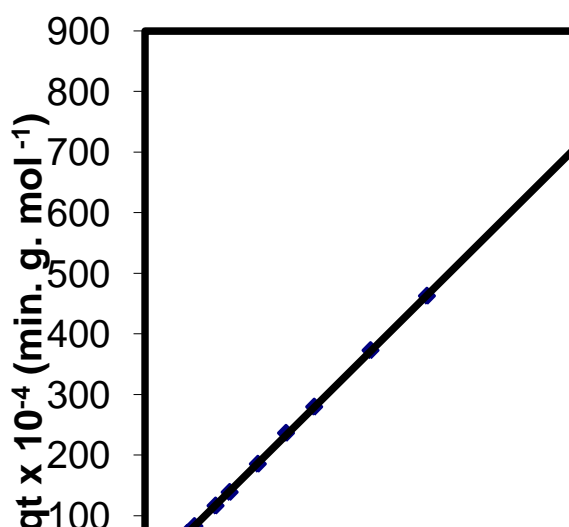


Fig. 7: Pseudo second order plot for Mn (II) biosorption onto P. Ostreatus at pH 7 and at 298K.

Equilibrium Adsorption Studies of Mn (II) by P. Ostreatus

Effect of pH

The adsorption of Mn (II) on P. Ostreatus is carried out in pH range 3 to 8 at 298 K (Fig. 8). The Mn (II) biosorption onto P. Ostreatus is lower in the acidic pH range and increases with the increase in pH. Below PZC (6.5) the surface of P. Ostreatus is charged positively due to protonation of carboxyl, amine and alcoholic groups whereas the surface is negatively charged above its PZC value. In the pH range above PZC (*i.e.* alkaline pH range) coulombic forces of attraction between the negative surface and the positive Mn (II) ions results in increase in adsorption of Mn (II) onto the surface of P. Ostreatus. Below PZC the repulsive forces between the

positively charged surface of P. Ostreatus and Mn (II) cations is responsible for the decrease in the uptake of Mn (II) ions onto P. Ostreatus. The decrease in equilibrium pH values with increase in metal ion sorption indicates that cation exchange mechanism is responsible for the uptake of Mn (II) by P. Ostreatus. Moreover, the lower sorption in acidic pH range may also be due to the competition between hydrogen ions and positive Mn (II) ions for the same surface sites of the sorbent. Similar results were recorded for the uptake of Mn (II) onto the crab shells particles as a function of pH [7].

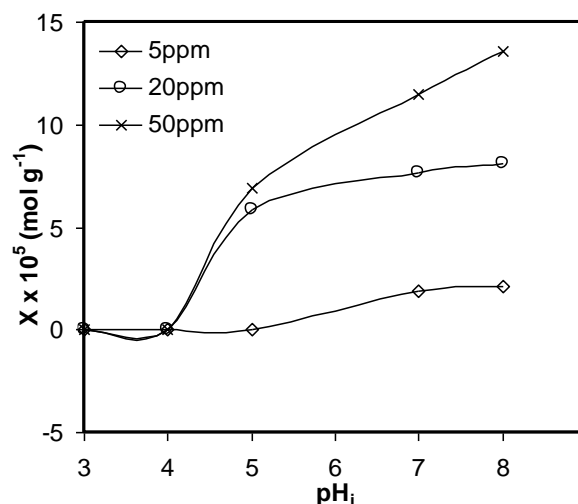


Fig. 8: Effect of pH on Mn (II) biosorption by P. Ostreatus at 298 K.

Effect of Temperature

The adsorption of Mn (II) onto the P. Ostreatus was carried out at 298, 308, 318 and 328 K. As is obvious from the Fig. 9 the uptake of Mn (II) onto P. Ostreatus decreases with the increase in temperature indicating the exothermic nature of the process. The adsorption of Mn (II) onto P. Ostreatus decreases from 19.6×10^{-5} at 298 K to 16×10^{-5} mol g⁻¹ at 328 K. This decrease in adsorption may be attributed to the change in configuration of the cell wall surface with increase in temperature. As expected, several surface sites get destroyed with heat, decreasing the sorption capacity of Mn (II) onto P. Ostreatus. Another reason may be the weakening of binding forces between surface of sorbent and metal ions with the increase in temperature of the system and at high temperature the tendency of metal ions increase to escape from the surface. Similar

results were reported for the adsorption of Ni (II) by immobilized cells of bacillus species [30].

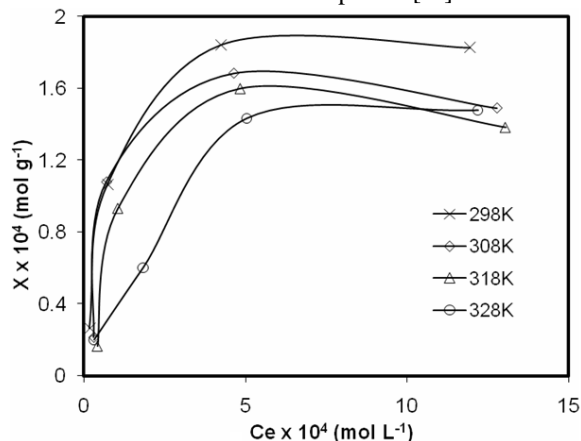


Fig. 9: Effect of temperature on Mn (II) biosorption by P. Ostreatus at different temperatures and at pH 6.

Langmuir Model

The current data was subjected to the well known Langmuir model which assumes that adsorption is reversible, monolayer and rules out the interaction between adsorbed metal concentrations. Its linear form is given below

$$\frac{Ce}{X} = \frac{1}{KX_m} + \frac{Ce}{X_m} \quad (2)$$

where Ce is the remaining concentration, X (mol g^{-1}) is the adsorbed amount, X_m is the maximum adsorbed amount, K_b is the binding energy constant. The values of X_m and K_b were calculated from graph plotted between $\frac{Ce}{X}$ vs. Ce (Fig. 10) with

high correlation of coefficient *i.e.* > 0.95 . Both the values of X_m and K_b (Table-2) decrease with the increase in temperature indicating the exothermic nature of the process [31]. The values of binding energies fall within the range ($13803 - 3659 \text{ L g}^{-1}$). Similar results were reported for the adsorption of Mn (II) by Pseudomonas [29]. The current values of X_m are higher than the adsorption capacities of other adsorbents (Table-3). From the above discussion, it is inferred that P. Ostreatus may be used effectively for the Mn (II) adsorption from aqueous solution.

Table-2: Langmuir parameters (X_m and K_b) for Mn (II) biosorption by P.Ostreatus at different temperatures and at pH 6

Temperature (K)	$X_m \times 10^5 (\text{mol g}^{-1})$	$K_b (\text{L g}^{-1})$
298	19.60	13803
308	16.30	11747
318	16.32	5768
328	18.53	3659

Table-3: Comparison of different biosorbents for sorption of Mn (II).

Alginate gel beads	3.64	Gotoh et al. (2004)
Carbon nanotube	<2.5	Stafiej et al. (2007)
Kaolinite	0.442	Yauvz et al. (2003)
Agaricus bisporous	3.64	Sesli and Tuzen (1999)
Bolliyus edulis	2.9	Tuzen et al. (1998)
Russula delica	9.6	Yilmaz et al. (2003)
P.Ostreatus	10.1	Present work

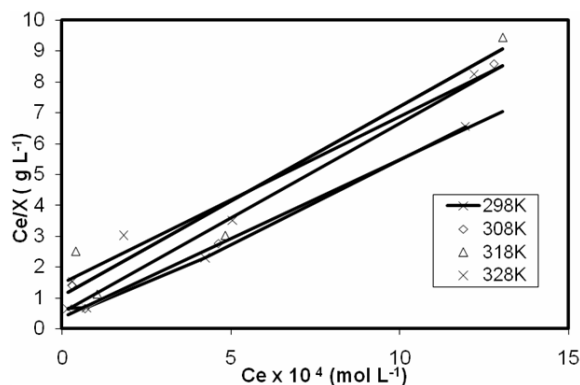


Fig. 10: Langmuir plots for Mn (II) biosorption by P. Ostreatus at different temperatures and at pH 6.

Thermodynamic Parameters

The change in enthalpy (ΔH) and entropy (ΔS) were calculated from the plot of $\ln K_b$ vs $1/T$ (Fig. 11) according to equation 3.

$$\ln K_b = \frac{\Delta S}{R} - \frac{\Delta H}{RT} \quad (3)$$

where K_b is the Langmuir parameter. The Gibbs free energy values were computed from the following mathematical expression.

$$\Delta G = \Delta H - T\Delta S \quad (4)$$

The thermodynamic parameters for sorption of Mn (II) onto P. Ostreatus are given in Table-4. The

negative values of ΔG (-23.93 – -22.51 kJ mol⁻¹) show the feasibility of the adsorption process and further indicate that sorption forces are strong enough to break the barrier for Mn (II) adsorption onto *P. Ostreatus*. The decrease in the negative ΔG values with increase in temperature shows a decline in spontaneity which indicates the process of the adsorption is not favorable at high temperature. Similar ΔG values were reported previously by [32]. The negative value of ΔH (-37.9 kJ mol⁻¹) shows the exothermic nature of the Mn (II) sorption onto *P. Ostreatus*. Similar ΔH value was also observed by [31] while studying the biosorption of cadmium by coconut copra. Moreover the value of ΔS (J mol⁻¹ k⁻¹) is observed to be negative which reveals less randomness at the solid liquid interface. The present value is closer to the value of ΔS (-13 J Mol⁻¹ k⁻¹) reported by [33], while studying adsorption of Mn (II) by comcob biomass.

Table 4: Thermodynamic parameters for Mn (II) biosorption on *P. ostreatus* at different temperatures and at pH 6.

$X \times 10^4 (\text{mol g}^{-1})$	$\Delta H (\text{kJ mol}^{-1})$	R^2
1.4	-29.12	0.92
1	-35.02	0.79
0.8	-50.62	0.82
0.6	-64.39	0.86

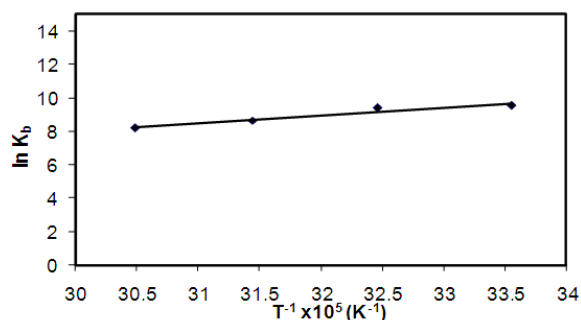


Fig. 11: Plot of $\ln K_b$ vs. $1/T$ for biosorption of Mn (II) by *P.Ostreatus* at pH 6.

Isosteric Heat of Adsorption

Isosteric heat of adsorption gives important information about sorbate - sorbent interaction at a constant amount of adsorbed Mn (II) ions and also about the nature of the surface of sorbent. The Clausius-Clapeyron equation was used to calculate isosteric heat ($\overline{\Delta H}$) of adsorption.

$$\ln [C_e]_{\theta} = \frac{\Delta H}{RT} + K \quad (5)$$

where C_e (mol L⁻¹) represents the equilibrium concentration after adsorption, θ represent the constant amount of adsorbed Mn (II) ions on the surface and R is the gas constant (8.314 J mol⁻¹). The isosteric heat of adsorption ($\overline{\Delta H}$) is calculated from the slope of a plot between $(\ln C_e)_{\theta}$ vs. $1/T$ Fig. 12. The isosteric heat of adsorption at constant surface loading is given in Table-5. The negative value of $\overline{\Delta H}$ confirms the exothermic nature of Mn (II) adsorption onto *P. Ostreatus*. Moreover, the variation in $\overline{\Delta H}$ values indicates that the surface remains energetically heterogeneous. The values of $\overline{\Delta H}$ decrease with the increase in surface loading (θ) (Fig. 13) which is probably because of the lateral interactions between the adsorbed metal ions which results in the decrease in the isosteric heat of adsorption. Moreover, the current negative values of isosteric heat of adsorption further aguments the conclusion drawn from the enthalpy of adsorption and decrease in the ΔG values with the rise in temperature. Similar variation in ($\overline{\Delta H}$) with the change in surface loading was reported by [34] for zinc uptake by olive oil mill solid residues.

Table-5: Isosteric heat of Mn (II) biosorption on *P. Ostreatus* at pH 6.

Temp (K)	ΔG (kJ mol ⁻¹)	ΔH (kJ mol ⁻¹)	ΔS (J mol ⁻¹ K ⁻¹)
298	-23.92	-37.96	-47
308	-23.45		
318	-22.98		
328	-22.51		

P. Ostreatus at pH 6.

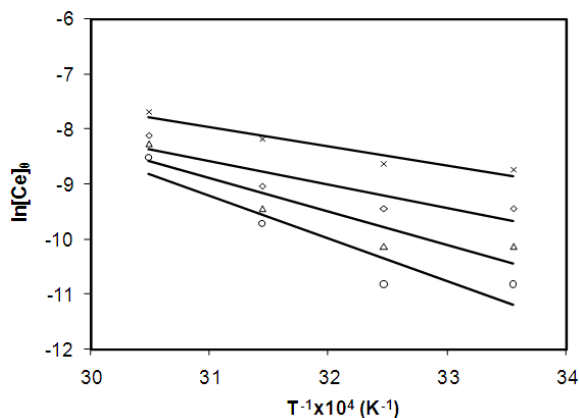


Fig. 12: Plot of $\ln[Ce]_{\theta}$ vs. T^{-1} for Mn (II) biosorption onto P. Osreatus at pH 6.

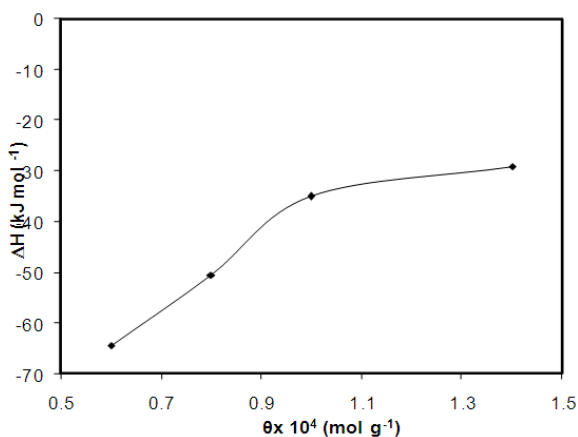


Fig. 13: Isosteric heat (ΔH) as a function of surface coverage $[\theta]$ for Mn (II) biosorption onto P.Ostreatus.

FTIR Studies

The solid residue of P. Ostreatus before and after adsorption was characterized by FTIR. Fig. 4(B) shows a change in the absorption band at around 1600 – 1650 cm^{-1} after adsorption of Mn (II) onto the surface. The change in adsorption bands in IR spectra after adsorption of Mn (II) onto P.Ostreatus is due to the binding of Mn (II) ions onto carbonyl (C = O) groups available on the surface. Similar changes in the FTIR spectrum was reported by Xiangliang et al., (2005) for Pb (II) sorption by P. Ostreatus. Moreover, similar change in IR spectra was also observed by [35], for Mn (II) adsorption by thermally decomposed leaf.

Experimental

Chemicals and Reagents

Common laboratory glasswares were used during adsorption experiments. All glasswares were thoroughly washed with deionized water. All chemicals were of analytical grade. Initially 1000 mg L^{-1} stock solution of manganese was prepared in a deionized water. The working solutions of desired concentrations of Mn (II) ranging from 5 to 250 mg L^{-1} were prepared for further experimental work.

Preparation of Biosorbent

The fungus Pleurotus Ostreatus (P. Ostreatus) also called mushroom was purchased from local market in Peshawar city, Pakistan. It was thoroughly washed with tap water to remove the dust particles and water soluble impurities. The material was air dried in open sunlight for 48 h and was then dried in oven at 80 °C. The dried material without further processing was powdered and passed through 200 mm mesh. The dried sample of P. Ostreatus was characterized and was then effectively used for the Mn (II) adsorption.

Characterization

P.Ostreatus was characterized by scanning electron microscopy (SEM) model JSM 5910 JEOL. Elemental analysis was carried out by using EDX model INCA 200. The spectrum plotted between energy and intensity gave the weight and atomic percentage of elements present on the surface of fungus P. Ostreatus. The surface area was determined using the surface area analyzer model Quanta Chrome Nova 2200e. Prior to the analysis the sample was dried at 80 °C and then degassed at 100 °C for about 1 h. Brnauer- Emmett-Teller (BET) model was tested to assess the surface area of P. Ostreatus. The powder sample of P. Ostreatus was subjected to XRD analysis using the X. ray diffractometer model JDX- 3532 to determine the geometry of the material. Thermal analyses of the P. Ostreatus were performed by thermogravimetric and differential thermal analyzer model Perkin Elmer 6300. Weighted sample was subjected to the thermal analysis under control heating and the heating rate was 10 °C min^{-1} . Heating of sample was done in the temperature range of 30 – 1000 °C. Furnace model N71H Naberthem with the program controller was used to determine weight loss of sample. The change in weight was calculated from difference in weight of the P. Ostreatus before and after heating.

Infrared spectrometer model Shimadzu 8201 PC was used for FTIR analysis of P. Ostreatus. The sample was mixed with KBr in 1:100 ratios. Before FTIR analysis the sample was desiccated for 24 h. The PZC of P. Ostreatus was determined by salt addition method. Fourty millimeter of 0.1M NaNO_3 solution was mixed with 0.1 g of adsorbent in different flasks. The initial pH was adjusted by using 0.1M HCl / NaOH solutions. Initial pH was recorded using pH meter model Boeche BT- 600 (Germany). The suspensions were equilibrated in Wise Bath shaker at 120 rpm for 24 hrs at 298 K. The final (pH_f) was noted. The ΔpH (difference between final and

initial pH) were plotted vs. initial (pH_i). The pH_i where ΔpH was zero was considered to be the PZC of *P. Ostreatus*.

Sorption Studies

Batch biosorption experiments were conducted in 100 ml conical flask with 0.1 gm of biosorbent and 40 ml of Mn (II) solutions. The pH of the system was adjusted in the range of 2 to 8. These flasks were then equilibrated in a Wise bath shaker at 120 rpm for 24 hrs at 298 K. Suspensions were then filtered and the filtrates were analyzed. The amount of metal ions in the filtrates was determined using Perkin Elmer A Analyst 800 atomic absorption spectrometer. The adsorption studies were conducted at 298, 308, 318 and 328 K. The amount of Mn (II) adsorbed was determined from the difference between initial and final concentration. The solid residue before and after Mn (II) adsorption was characterized by FTIR and SEM/EDX.

Conclusions

The kinetic study showed that 3 hours are enough for the Mn (II) adsorption onto *P. Ostreatus*. The pseudo 2nd order model was best applicable to the experimental data. The Mn (II) biosorption onto the surface of *P. Ostreatus* was found to increase with increase in pH while a decrease in the adsorption of Mn (II) onto the surface of *P. Ostreatus* was observed with temperature. The batch adsorption data was well fitted to the Langmuir model with a high correlation coefficient. Both X_m and K_b values decrease with elevation in the temperature of the system. All thermodynamic parameters were found to be negative showing the system to be spontaneous and exothermic in nature with a decreased randomness at the surface of the sorbent respectively. The variation in the isosteric heat of adsorption with variation in surface loading indicates the heterogeneous nature of adsorbent.

Finally it was concluded that *P. Ostreatus* behaves as a suitable biosorbent for the decontamination of water from the Mn (II) ions.

References

1. M. Waseem, S. Mustafa and A. Naeem, *Journal of the Chemical Society of Pakistan*, **33**, 619 (2011).
2. M. Hamayun, T. Mahmood, A. Naeem, M. Muska, S. U. Din and M. Waseem, *Chemosphere*, **99**, 207 (2014).
3. T. Mahmood, S. U. Din, A. Naeem, S. Tasleem A Alum, and S. Mustafa, *Journal of Industrial and Engineering Chemistry*, **20**, 3234 (2014).
4. S. Mustafa, M. Safdar, M. Waseem, A. Naeem, S. Tasleem, K. H. Shah and M. T. Jan, *Journal of the Chemical Society of Pakistan*, **33**, 619 (2011).
5. A. Naeem, M. T. Saddique, S. Mustafa, S. Tasleem, K. H. Shah and M. Waseem, *Journal of Hazardous Materials*, **172**, 124 (2009).
6. T. Mahmood, S. U. Din, A. Naeem, S. Mustafa, M. Waseem and M. Hamayun, *Chemical Engineering Journal*, **192**, 90 (2012).
7. K. Vijayaraghavan, H. Y. N. Winnie and R. Balasubramanian, *Desalination*, **266**, 195 (2011).
8. A. A. Mengistie, T. S. Rao and A. V. P. Rao, *Global Journal of Science Frontier Research Chemistry*, **12**, 2249 (2012).
9. V. J. P. Vilar, S. C. R. Santos, R. J. E. Martins, C. M. S. Botelho and R. A. R. Boaventura, *Biochemical Engineering Journal*, **42**, 276 (2011).
10. Z. Imaizumi, S. T. Katsumi, T. I. X. Tang and Q. Tang, *Journal of Hazardous Materials*, **177**, 501 (2010).
11. M. U. Haq, R. A. Khattak, H. K. Puno, M. S. Saif, K. S. Memon, *International Journal of Agriculture and Biology*, **7**, 214 (2005).
12. S. Mahmood and A. Maqbool, *Pakistan Journal of Water Resources*, **10**, 19 (2006).
13. A. Azizullah, M. N. K. Khattak, P. Richter and D. Häder, *Environment International*, **37**, 479 (2011).
14. A. K. Bhattacharyya, T. K. Naiya, S. N. Mandal and S. K. Das, *Chemical Engineering Journal*, **137**, 529 (2008).
15. S. Naeem, U. Zafar, A. Altaf and A. Inayat, *Journal of Chemical Society of Pakistan*, **31**, 379 (2009).
16. D. B. A. Fil and C. Özmetin, *Journal of Chemical Society of Pakistan*, **34**, 896 (2012).
17. T. M. Yagub, K. T. Sen and H. M. Ang, *Water Air Soil Pollution*, **223**, 5267 (2012).
18. J. C. M. Pirajan, V. S. G. Cuello and L. Giraldo, *Adsorption*, **17**, 505 (2011).
19. N. S. Maurya, A. K. Mittal, P. Cornel and E. Rother, *Bioresource Technology*, **97**, 512 (2006).
20. N. Das, *Natural Product Radiance*, **4**, 454 (2005).
21. C. C. H. Tay, H. Liew, C. Yin, S. Talib, S. Surif, A. A. Suhaimi and S. K. Yong, *Korean Journal of Chemical Engineering*, **28**, 825 (2010).
22. C. Islek, A. Sinag, and I. Akata, *Clean*, **36**, 387 (2008).

23. K. Swayampakula, V. Boddub, S. K. Nadavala and K. Abburia, *Journal of Hazardous Materials*, **170**, 680 (2009).
24. L. Odochian, C. Moldoveanu, A. M. Mucanu and G. Carja, *Thermochimica Acta*, **526**, 205 (2011).
25. X. Yang, Y. Zeng, F. Ma, X. Zhang and H. Yu, *Bioresource Technology*, **101**, 5475 (2010).
26. P. Xiangliang, W. Jianlong and Z. Daoyong, *Process Biochemistry*, **40**, 2799 (2005).
27. T. Mahmood, M. T. Saddique, A. Naeem, P. Westerhoff, S. Mustafa and A. Alum, *Industrial and Engineering Chemistry Research*, **50**, 10017 (2011).
28. M. E. Fernandez, G. V. Nunell, P. R. Bonelli and A. L. Cukierman, *Bioresource Technology*, **101**, 9500 (2010).
29. D. Gialamouidis, M. Mitrakes and M. L. Kyriakides, *Journal of Hazardous Materials*, **182**, 672 (2010).
30. A. Tahir, R. Shehzadi, B. Mateen, S. Univerdi and O. Karacoban, *Engineering in Life Sciences*, **9**, 462 (2009).
31. Y. Hoa and A. E. Ofomaja, *Biochemical Engineering Journal*, **30**, 117 (2006).
32. B. Y. M. Bueno, M. L. Torem, R. J. Carvalho, G. A. H. Pino and L. M. S. Mesquita, *Minerals Engineering*, **24**, 1619 (2011).
33. A. I. Adeogun, A. E. Ofudje, M. Kareem and O. Sarafadeen, *Bioresource Technology*, **6**, 4117 (2011).
34. A. Hawari, Z. Rawajfih and N. Nsour, *Journal of Hazardous Materials*, **168**, 1284 (2011).
35. Z. Li, S. Imaizumib, T. Katsumia, T. Inuia, X. Tangc and Q. Tangc, *Journal of Hazardous Materials*, **177**, 501 (2010).